28th European Young Geotechnical Engineers Conference – EYGEC 2024

Geogrid Reinforced Soil Model Calibration Based on Laboratory Testing

Mindaugas Zakarka[a], Šarūnas Skuodis[a], Johannes Kuhlmann[b]

[a] *Department of Reinforced Concrete Structures and Geotechnics, Vilnius Gediminas Technical University, Vilnius, Lithuania*
[b] *Chair of Geotechnical Engineering, Department of Civil Engineering, University of Siegen, Siegen, Germany*

ABSTRACT

Geogrids are widely applied in infrastructure projects to enhance load-bearing capacity and mitigate soil settlement. Understanding the behaviour of soil reinforced with geogrids is crucial for optimizing design practices. This study investigates the mechanical properties of sand samples reinforced with geogrids through laboratory testing and numerical simulations. Triaxial compression tests were conducted for unreinforced and geogrid-reinforced sand samples with a variable confining pressures. The tests revealed an increase in cohesion (apparent cohesion) and minimal change in the angle of internal friction with geogrid reinforcement. Numerical simulations using the Hardening Soil model in PLAXIS 3D were performed to replicate laboratory tests, with adjustments made to improve alignment between numerical and experimental results. The numerical simulations demonstrated good agreement with laboratory-derived deviator peak values, with minor discrepancies observed at low cell pressures. Adjustments to the power index (m) and ultimate stiffness modulus (E_{ur}) were necessary to achieve better alignment, particularly regarding deformations at which the deviator peak occurred. The study concludes that the modelling approach is suitable for accurate triaxial compression tests simulations for soils reinforced with geogrids. The findings contribute to the advancement of geotechnical engineering practices, facilitating more accurate design and analysis of geogrid-reinforced structures.

KEYWORDS

Geogrid reinforcement; Hardening soil model; Triaxial compression test; Numerical simulation.

1. INTRODUCTION

Geogrids are widely utilized in various infrastructure projects to enhance load-bearing capacity and reduce soil settlement (Bhardwaj and Mittal, 2022). Their application aims to improve mechanical properties, which are crucial for ensuring the stability and durability of engineered structures (Zornberg, 2017). Understanding the behaviour of soil reinforced with geogrids is essential for optimizing design and construction practices, prompting extensive research efforts employing numerical simulations, analytical methods, laboratory experiments, and in situ investigations (Makkar, 2019; Zakarka and Skuodis, 2024).

Numerical analysis has become a prevalent tool in geotechnical engineering, offering insights into complex soil-structure interactions and aiding in the optimization of engineering projects (Ikeagwuani and Nwonu, 2019). Constitutive soil models play a pivotal role in numerical simulations, allowing for the representation and prediction of stress-strain behaviour under varying conditions. Among these models, the Hardening Soil model has demonstrated accuracy in simulating triaxial compression test behaviour (Pacheco et al., 2021).

However, the accuracy of numerical simulations heavily relies on the quality of input parameters derived from laboratory or field tests (Konyushkov et al., 2023; Lankaran et al., 2022). Model calibration is often necessary to ensure accurate representation of soil behaviour in numerical models (Calvello and Finno, 2004). While Mohr-Coulomb strength parameters (c' and φ') are well-established for

unreinforced soils (Wu and Tung, 2020), challenges persist in determining mechanical properties for geogrid-reinforced soils (Zakarka et al., 2023).

In particular, understanding compressibility is crucial for accurately simulating deformations in numerical models like PLAXIS 3D. The power index *m* is a key parameter influencing compressibility, with recommendations varying for different soil types: 0.5 for Norwegian sands and silts (Janbu, 1963), 1.0 for normally consolidated clay (Surarak et al., 2012), 0.45 for rockfill material (Honkanadavar and Sharma, 2016). However, specific recommendations for geogrid-reinforced soils remain scarce, highlighting the need for further investigation.

This study aims to address this gap by conducting consolidated drained (CD) triaxial compression tests on unreinforced sand and sand reinforced with geogrid across a wide range of confining pressures (20, 50, 70, 100, 200, 300 kPa). The obtained parameters will be utilized to simulate laboratory tests using the Hardening Soil model in PLAXIS 3D. By comparing the simulation results with laboratory findings, this research seeks to determine the suitability of existing recommendations for simulating triaxial compression tests for geogrid-reinforced soils.

2. MATERIAL AND METHOD

2.1. Soil Material

The material utilized for this investigation was sand (SaU), conforming to LST EN ISO 14688-2 (Lithuanian Standards Board, 2020). It exhibited a uniformity coefficient (C_U) of 2.25, curvature coefficient (C_C) of 1.08, and an average particle size (d_{50}) of 0.19 mm. The particle size distribution is presented in Figure 1. To ensure consistent testing conditions, soil samples were carefully prepared by recompaction to reach optimal density at the optimal water content, as determined by Proctor compaction testing (Lithuanian Standards Board, 2015). The optimal water content was found to be 14.3%, resulting in a bulk density of the prepared sample of 1.86 g/cm^3.

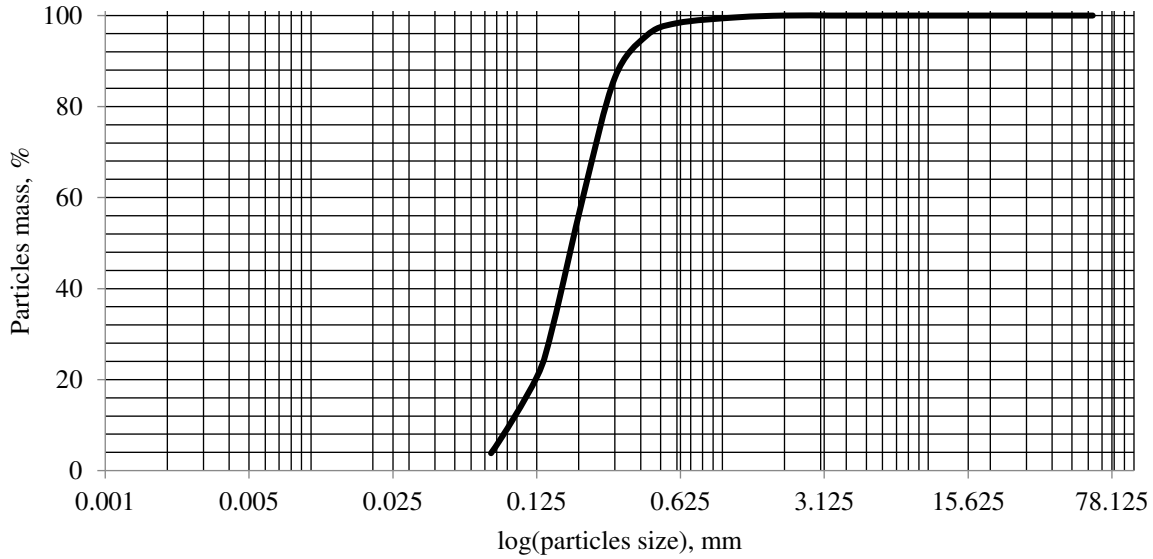

Figure 1. Particle size distribution curve

2.2. Geogrid Reinforcement

Flexible polyester (PET) geogrid with a mesh size of 25 × 25 mm and an ultimate tensile strength of 40 kN/m was employed to reinforce the soil samples. The geogrid was carefully cut into circles with diameters 3-5 mm smaller than the soil sample's diameter (100 mm), as illustrated in Figure 2, to prevent potential membrane damage.

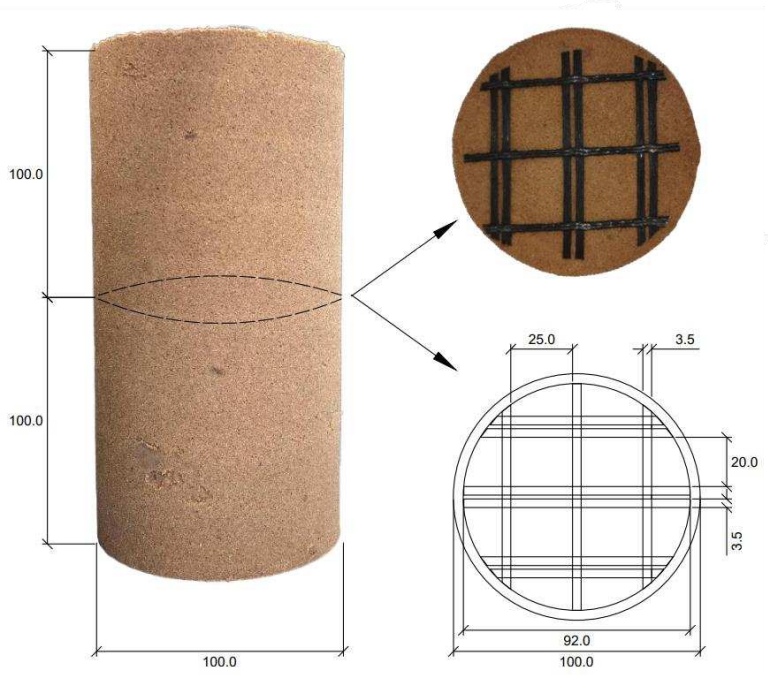

Figure 2. Preparation of the samples example used in the triaxial cell: (left) – prepared soil sample, (right) – geogrid top view in the middle of the sample

2.3. Specimen Preparation

Two types of cylinder specimens were prepared for triaxial compression testing: unreinforced soil and soil reinforced with a single layer of geogrid positioned at the center of the sample. Each specimen had a diameter of 100 mm, and a height of 200 mm. Remolding was achieved through 10 layers at the optimal water content to achieve optimal density.

2.4. Triaxial Compression Testing

Consolidated drained (CD) triaxial compression tests were conducted, initially on soils without geogrid reinforcement, followed by tests on geogrid-reinforced soils. Six different cell pressures (σ_3) were applied during consolidation and loading phases: 20, 50, 70, 100, 200, and 300 kPa. Test conditions were selected in accordance with LST EN ISO 17892-9:2018 (Lithuanian Standards Board, 2018). The consolidation period was set at 30 minutes, with the rate of vertical displacement of the load frame adjusted to 0.95%/min. The test concluded upon loading the specimen up to 15% of vertical deformation.

2.5. Numerical Simulation

Finite element method (FEM) and the SoilTest module of PLAXIS 3D software were employed to model the triaxial compression tests. The Hardening Soil Model (HS) was utilized to simulate the tests, based on plasticity theory, where the stress-strain relationship due to primary load is hyperbolic (Brinkgreve and PLAXIS BV, 1999). The ultimate deviatoric stress (q_f) was determined using the Mohr-Coulomb criterion:

$$q_f = \frac{2\sin\varphi'}{1-\sin\varphi'}(\sigma_3' + c' \cdot \cot\varphi') \quad (1)$$

where c' and φ' are the effective shear strength parameters and σ_3' is the confining stress in the cell.

The confining stress-dependent stiffness modulus (E_{50}) was calculated:

$$E_{50} = E_{50}^{ref} \left(\frac{\sigma_3' + c' \cdot \cot \varphi'}{p^{ref} + c' \cdot \cot \varphi'} \right)^m \quad (2)$$

where E_{50}^{ref} is the reference secant stiffness modulus to be determined from the drained triaxial test, p^{ref} is the reference isotropic stress where a default value equal to 100 kPa is recommended by the software.

The power index m is the exponent that defines the strain dependence value of the stress state. The m value was obtained by Figure 3.

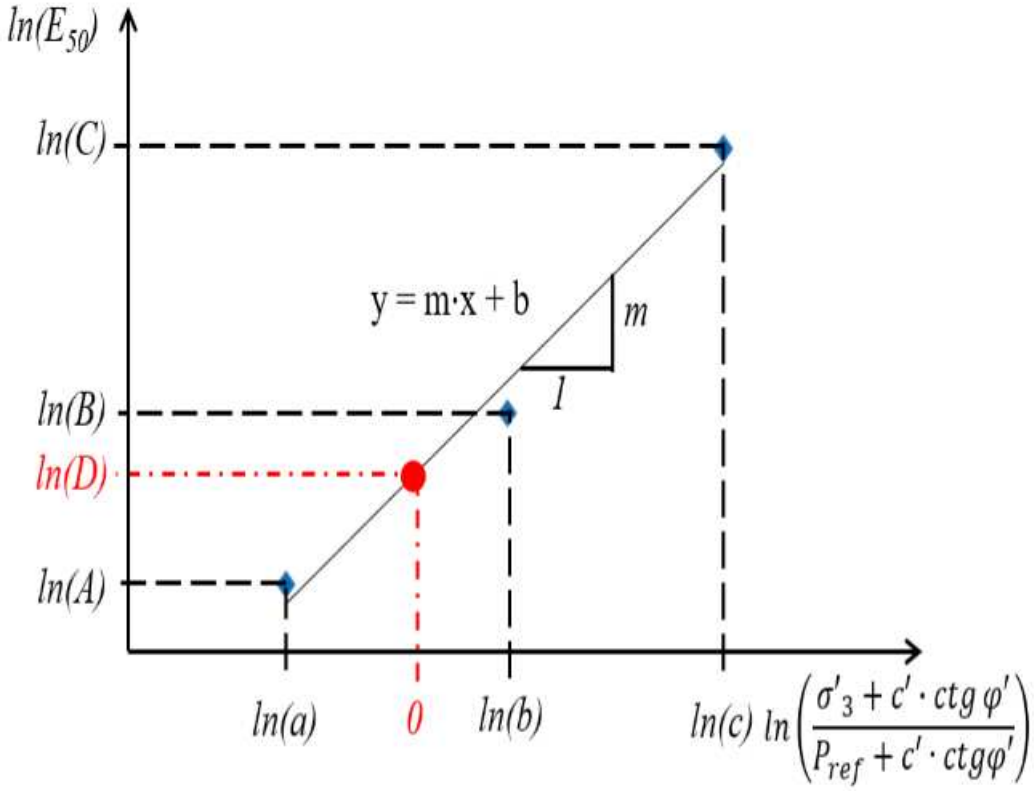

Figure 3. Determination of the Power Parameter m Graphically (Konyushkov et al., 2023)

where a trend line:

$$y = a \cdot x + b \quad (3)$$

where y:

$$y = \ln E_{50} \quad (4)$$

where x:

$$x = \ln \left(\frac{\sigma_3' + c' \cdot \cot \varphi'}{p^{ref} + c' \cdot \cot \varphi'} \right) \quad (5)$$

Other necessary parameters for simulations were determined based on PLAXIS recommendations: E_{oed} equal to E_{50}, E_{ur} equal to $3E_{50}$, ν equal to 0.3, K_0^{nc} equal to $1-\sin \varphi'$ for normally consolidated soils.

3. RESULTS

3.1. Laboratory Testing Results

Interpretation of the results was carried out using the Mohr-Coulomb criterion. For soil samples without geogrid reinforcement, the angle of internal friction (φ) was determined to be 40.67°, with a cohesion c of 0.66 kPa. In contrast, soil samples reinforced with geogrid exhibited an angle of internal friction of 40.93° and a cohesion of 12.62 kPa. The secant stiffness modulus E_{50} values ranged from 17.62 to 90.42 MPa for soil without geogrid reinforcement and from 16.04 to 86.37 MPa for soil with geogrid reinforcement (see Table 1). Additionally, power indexes m were determined as 0.5853 for soil without geogrid and 0.6194 for soil with geogrid (see Figure 4), facilitating the determination of corresponding E_{50}^{ref} values (see Table 1). The average E_{50}^{ref} values were 44.71 MPa for soil without geogrid reinforcement and 49.27 MPa for soil with geogrid reinforcement.

Table 1. Results of Secant Stiffness E_{50} and Power Indexes m

Cell pressure, kPa	Without geogrid			With geogrid		
	Secant stiffness, MPa		Power index	Secant stiffness, MPa		Power index
	E_{50}	E_{50}^{ref}	m	E_{50}	E_{50}^{ref}	m
20	17.62	45.33	0.5853	16.04	42.34	0.6194
50	34.01	51.07		38.24	58.35	
70	32.87	40.51		43.25	53.79	
100	38.03	38.03		44.97	44.97	
200	68.75	45.80		79.93	52.20	
300	90.42	47.51		86.37	43.93	
Average		44.71			49.27	

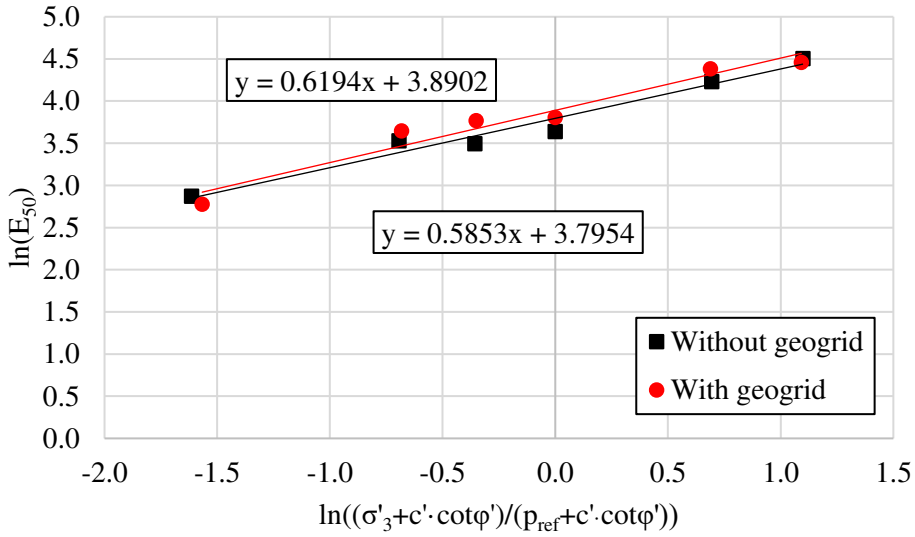

Figure 4. Determination of Power Indexes m for Soil Samples with and without Geogrid Reinforcement

3.2. Numerical Simulations Results

The deviator peak determined by the laboratory tests exceeded that obtained through modelling, particularly evident at a cell pressure of 20 kPa, where discrepancies reached 27.32% for soil without geogrid and 10.06% for soil with geogrid (see Table 2). Although better agreement was observed at higher cell pressures, differences still existed, ranging from -8.67% to 7.75% for soil without geogrid and from -11.85% to 3.53% for soil with geogrid. Significant disparities were also noted in the deformations at which the deviator peak occurred (see Table 2). While laboratory tests indicated variations from 2.85% to 4.75% for soil without geogrid and from 3.33% to 4.80% for soil with geogrid, modelling yielded a wider range, from 2.10% to 6.00% and from 2.85% to 6.15%, respectively.

Table 2. Results of Deviator Peak (σ_1-σ_3) and Vertical Deformation $(\varepsilon_1)_{100}$ at which the Deviator Peak Occurred

Without geogrid

Cell pressure, kPa	Deviator peak σ_1-σ_3, kPa			Vertical def. $(\varepsilon_1)_{100}$, %		
	Experimental	Numerical	Difference	Experimental	Numerical	Difference
20	106.94	77.73	-27.32	2.85	2.10	-26.30
50	208.04	190.00	-8.67	3.38	2.70	-20.13
70	275.35	264.85	-3.81	3.32	3.90	17.40
100	356.29	377.13	5.85	4.11	4.65	13.02
200	697.33	751.37	7.75	4.13	5.10	23.36
300	1147.01	1125.63	-1.86	4.74	6.00	26.53
With geogrid						
20	145.98	131.29	-10.06	3.33	2.85	-14.31
50	244.19	245.28	0.45	3.41	3.30	-3.13
70	364.48	321.28	-11.86	3.48	3.90	12.17
100	443.51	435.27	-1.86	4.30	4.20	-2.30
200	863.70	815.24	-5.61	4.43	5.40	21.81
300	1154.49	1195.21	3.53	4.80	6.15	28.18

3.3. Parameter Adjustments for Improved Fit

The initial simulations yielded discrepancies in the deformations at which the deviator peak occurred, prompting the need for calibration. To achieve better alignment between laboratory tests and simulation results, iterative adjustments were made to the power index m and ultimate stiffness modulus E_{ur}. Specifically, the values of the power index m and E_{ur} were iteratively adjusted until the simulated deformations closely matched those observed in the laboratory tests. Optimal values of m equal to 0.8 were determined for both soil with and without geogrid, while E_{ur} was set to 3.5 times E_{50} for soil without geogrid and 6 times E_{50} for soil with geogrid. These adjustments resulted in vertical deformations at which the deviator peak occurred varying from 2.85% to 4.65% for soil without geogrid and from 3.15% to 4.80% for soil with geogrid (see Table 3). The final fit between laboratory tests and simulation is illustrated in Figure 5.

Table 3. Results of Vertical Deformations at which the Deviator Peak Occurred $(\varepsilon_1)_{100}$

Cell pressure, kPa	Without geogrid			With geogrid		
	Vertical def. $(\varepsilon_1)_{100}$, %					
	Experimental	Numerical	Difference	Experimental	Numerical	Difference
20	2.85	2.85	0.03	3.33	3.15	-5.29
50	3.38	3.30	-2.38	3.41	3.45	1.27
70	3.32	3.60	8.37	3.48	3.60	3.54
100	4.11	3.90	-5.21	4.30	3.90	-9.27
200	4.13	4.35	5.22	4.43	4.35	-1.88
300	4.74	4.65	-1.94	4.80	4.80	0.04

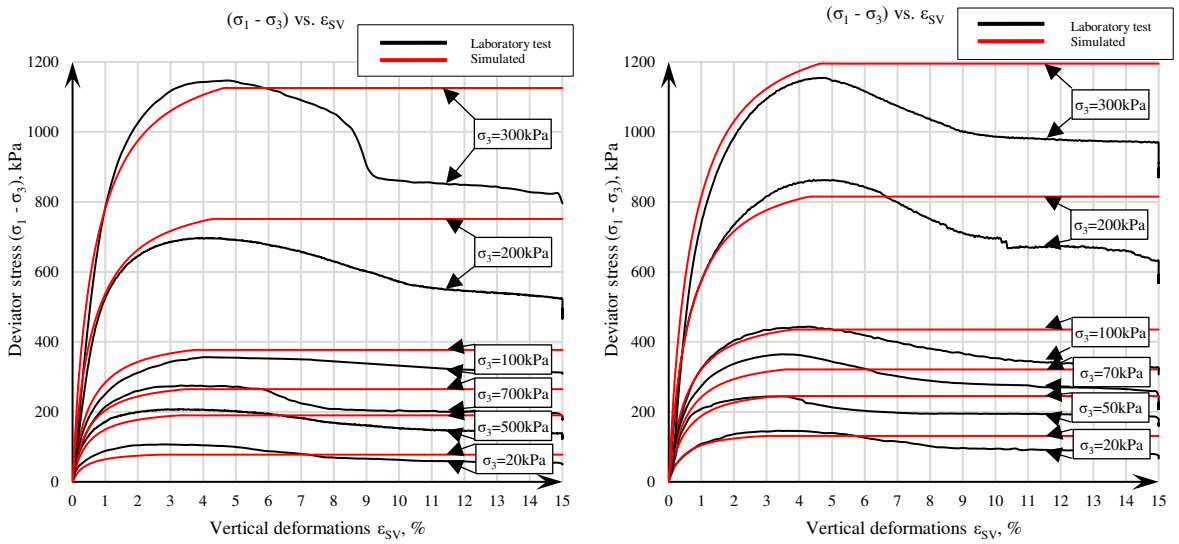

Figure 5. Deviator Stress and Vertical Deformations: (left) – for Soil Samples without Geogrid, (right) – for Soil Samples with Geogrid

The Hardening Soil model accurately simulates soil behaviour up to the deviator peak value, corresponding to vertical deformations ranging from 2.80% to 4.80%. However, it fails to model the post-peak behaviour due to limitations in capturing the residual shear strength, which is a crucial aspect for a comprehensive understanding of geogrid-reinforced soil behaviour.

4. CONCLUSIONS

Based on the findings derived from triaxial compression tests and modelling simulations, several key conclusions can be drawn:

1. Introduction of geogrid reinforcement into sand samples resulted in the creation of apparent cohesion (increasing from 0.66 kPa to 12.62 kPa), while the angle of internal friction exhibited minimal change (from 40.67° to 40.93°).

2. Modelling results demonstrated good agreement with laboratory-derived deviator peak values, with minor discrepancies observed primarily at low cell pressures (e.g., 20 kPa), where model-predicted values were slightly lower.

3. While initial modelling attempts using power index m values derived from triaxial compression tests provided satisfactory results for the deviator peak, adjustments to m and the ultimate stiffness modulus E_{ur} were necessary to achieve better alignment with laboratory test results, particularly regarding deformations at which the deviator peak occurred.

4. Notably, the modelling approach demonstrated no significant difference between soil samples with and without geogrid reinforcement, suggesting that the method is applicable for accurately modelling triaxial compression tests for soils reinforced with geogrids.

Overall, this study underscores the importance of both laboratory testing and modelling simulations in understanding the behaviour of geogrid-reinforced soils. The insights gained from this research contribute to the advancement of geotechnical engineering practices, facilitating more accurate design and analysis of geogrid-reinforced structures.

ACKNOWLEDGEMENT

This research was conducted during the ATHENA and Erasmus research programs, where the numerical simulations using PLAXIS 3D were performed. The conference participation was supported by the Center of Excellence project “Civil Engineering Research Centre” (Grant No. S-A-UEI-23-5).

REFERENCES

Bhardwaj, A., Mittal, S., 2022. Influence of Biaxial Geogrid at the Ballast Interface for Granular Earth Railway Embankment. Balt. J. Road Bridge Eng. 17, 1–20. https://doi.org/10.7250/bjrbe.2022-17.566

Brinkgreve, R.B.J., PLAXIS BV (Eds.), 1999. Beyond 2000 in computational geotechnics: ten years of PLAXIS International ; proceedings of the International Symposium Beyond 2000 in Computational Geotechnics, Amsterdam, the Netherlands, 18 - 20 March 1999. Presented at the International Symposium Beyond 2000 in Computational Geotechnics, Balkema, Rotterdam.

Calvello, M., Finno, R.J., 2004. Selecting parameters to optimize in model calibration by inverse analysis. Comput. Geotech. 31, 410–424. https://doi.org/10.1016/j.compgeo.2004.03.004

Honkanadavar, N.P., Sharma, K.G., 2016. Modeling the triaxial behavior of riverbed and blasted quarried rockfill materials using hardening soil model. J. Rock Mech. Geotech. Eng. 8, 350–365. https://doi.org/10.1016/j.jrmge.2015.09.007

Ikeagwuani, C.C., Nwonu, D.C., 2019. Emerging trends in expansive soil stabilisation: A review. J. Rock Mech. Geotech. Eng. 11, 423–440. https://doi.org/10.1016/j.jrmge.2018.08.013

Janbu, N., 1963. Soil compressibility as determined by oedometer and triaxial tests. Proc ECSMFE 1, 19–25.

Konyushkov, V., Penkov, D., Fedorenko, E., 2023. Initial data for Hardening Soil model. E3S Web Conf. 371, 02019. https://doi.org/10.1051/e3sconf/202337102019

Lankaran, Z.E., Nik Daud, N.N., Rostami, V., Yusoff, Z.Md., 2022. Consolidated Drained Triaxial Test on Treated Coastal Soil and Finite Element Analysis Using PLAXIS 2D. Adv. Mater. Sci. Eng. 2022, 1–15. https://doi.org/10.1155/2022/7263333

Lithuanian Standards Board, 2020. Geotechnical Investigation and Testing—Identification and Classification of Soil—Part 2: Principles for a Classification.

Lithuanian Standards Board, 2018. Geotechnical Investigation and Testing—Laboratory Testing of Soil—Part 9: Consolidated Triaxial Compression Tests on Water Saturated Soils.

Lithuanian Standards Board, 2015. Unbound and Hydraulically Bound Mixtures—Part 2: Test Methods for Laboratory Reference Density and Water Content—Proctor Compaction.

Makkar, F.M., 2019. A Review on the Behaviour of Soil against Different Geosynthetic Interfaces. Presented at the International Conference on Geotechnics for High Speed Corridors, India.

Pacheco, K.W., Matheus, B.C., Pacheco, L.M., Sampa, N.C., Dienstmann, G., 2021. Analysis Of Araquari Sand Behavior Thought Numerical Modeling Of Triaxial Tests, Proceedings of the joint XLII Ibero-Latin-American Congress on Computational Methods in Engineering and III Pan-American Congress on Computational Mechanics, ABMEC-IACM, Rio de Janeiro, Brazil, November 9-12.

Surarak, C., Likitlersuang, S., Wanatowski, D., Balasubramaniam, A., Oh, E., Guan, H., 2012. Stiffness and strength parameters for hardening soil model of soft and stiff Bangkok clays. Soils Found. 52, 682–697. https://doi.org/10.1016/j.sandf.2012.07.009

Wu, J.T.H., Tung, S.C.-Y., 2020. Determination of Model Parameters for the Hardening Soil Model. Transp. Infrastruct. Geotechnol. 7, 55–68. https://doi.org/10.1007/s40515-019-00085-8

Zakarka, M., Skuodis, Š., 2024. Analysis of Soil-Geogrid Interaction and Alternative Soil Layer Approach for Improved Road Embankment Stability, in: Barros, J.A.O., Kaklauskas, G., Zavadskas, E.K. (Eds.), Modern Building Materials, Structures and Techniques, Lecture Notes in Civil Engineering. Springer Nature Switzerland, Cham, pp. 643–649. https://doi.org/10.1007/978-3-031-44603-0_66

Zakarka, M., Skuodis, Š., Dirgėlienė, N., 2023. Triaxial Test of Coarse-Grained Soils Reinforced with One Layer of Geogrid. Appl. Sci. 13, 12480. https://doi.org/10.3390/app132212480

Zornberg, J.G., 2017. Functions and Applications of Geosynthetics In Roadways. Procedia Eng. 189, 298–306. https://doi.org/10.1016/j.proeng.2017.05.048